Selective regulation of spontaneous activity of neurons of the deep cerebellar nuclei by N-type calcium channels in juvenile rats

Karina Alviña[1,2] and Kamran Khodakhah[1]

[1]*Dominick P. Purpura Department of Neuroscience, Albert Einstein College of Medicine, Bronx, NY 10461, USA*
[2]*Departmento de Ciencias Fisiológicas, Pontificia Universidad Católica de Chile, Santiago, Chile*

The cerebellum coordinates movement and maintains body posture. The main output of the cerebellum is formed by three deep nuclei, which receive direct inhibitory inputs from cerebellar Purkinje cells, and excitatory collaterals from mossy and climbing fibres. Neurons of deep cerebellar nuclei (DCN) are spontaneously active, and disrupting their activity results in severe cerebellar ataxia. It is suggested that voltage-gated calcium channels make a significant contribution to the spontaneous activity of DCN neurons, although the exact identity of these channels is not known. We sought to delineate the functional role and identity of calcium channels that contribute to pacemaking in DCN neurons of juvenile rats. We found that in the majority of cells blockade of calcium currents results in avid high-frequency bursting, consistent with the notion that the net calcium-dependent current in DCN neurons is outward. We showed that the bursting seen in these neurons after block of calcium channels is the consequence of reduced activation of small-conductance calcium-activated (SK) potassium channels. With the use of selective pharmacological blockers we showed that L-, P/Q-, R- and T-type calcium channels do not contribute to the spontaneous activity of DCN neurons. In contrast, blockade of high-threshold N-type calcium channels increased the firing rate and caused the cells to burst. Our results thus suggest a selective coupling of N-type voltage-gated calcium channels with calcium-activated potassium channels in DCN neurons. In addition, we demonstrate the presence of a cadmium-sensitive calcium conductance coupled with SK channels, that is pharmacologically distinct from L-, N-, P/Q-, R- and T-type calcium channels.

(Received 13 November 2007; accepted after revision 25 March 2008; first published online 27 March 2008)
Corresponding author K. Khodakhah: Department of Neuroscience, Albert Einstein College of Medicine, 1410 Pelham Parkway South, Kennedy Center, Room 506, Bronx, NY 10461, USA. Email: kkhodakh@aecom.yu.edu

A major function of the cerebellum is to coordinate movement and to maintain body posture and balance (Ito, 1984). The cerebellum consists of two anatomically distinct structures: the cortex and deep nuclei. The cerebellar cortex circuitry receives and integrates a large amount of sensory and cortical information. This information is relayed for further processing to neurons of the deep cerebellar nuclei (DCN).

As the main output of the cerebellum, the activity of DCN neurons encodes the cerebellar signals required for coordination of movement. Like most principal neurons involved in motor control, DCN neurons fire spontaneously (Jahnsen, 1986; Raman *et al.* 2000). Their output is generated by integrating synaptic inputs with their own intrinsic activity. Major alterations in the intrinsic activity of DCN neurons adversely affect cerebellar function causing ataxia (Shakkottai *et al.* 2004); therefore delineating the nature and functional role of the conductances contributing to the pacemaking of DCN neurons is essential to understanding the function of the cerebellum and its dysfunction in cerebellar ataxia.

Although the voltage-dependent calcium currents of DCN neurons are substantial (Gauck *et al.* 2001), they do not contribute to the depolarization between spikes (Raman *et al.* 2000). In fact, as a consequence of activation of calcium-activated potassium channels (K_{Ca}) the net calcium-dependent current is outward resulting in membrane hyperpolarization (Raman *et al.* 2000). Blockade of K_{Ca} channels in DCN neurons significantly increases both the rate of spontaneous activity and the number of evoked action potentials (Aizenman & Linden, 1999; Czubayko *et al.* 2001; Shakkottai *et al.* 2004). The physiological function of these channels is so significant

This paper has online supplemental material.

 DOI: 10.1113/jphysiol.2007.148197

that their selective genetic reduction in DCN neurons causes severe ataxia (Shakkottai *et al.* 2004). Thus, by virtue of activating K_{Ca} channels, voltage-gated calcium channels (VGCCs) significantly contribute to the pacemaking in DCN neurons.

Using specific blockers of VGCCs we find that blockade of only N-type, but not L-, P/Q-, R- or T-type calcium channels affects pacemaking of DCN neurons. Blockade of N-type calcium channels converts the tonic, regular activity of DCN neurons to high-frequency burst firing. This bursting is the consequence of the reduced activation of small-conductance K_{Ca} channels which regulate pacemaking in the majority of DCN neurons in juvenile rats. Additionally, we demonstrate the presence of a cadmium-sensitive calcium conductance coupled with SK channels which is pharmacologically distinct from N-, L-, P/Q-, R- and T-type calcium channels.

Methods

Slices

All procedures employed were in accordance with the policies established by the Animal Institute Committee of the Albert Einstein College of Medicine. Wistar rats (P 12–20) were anaesthetized with halothane and decapitated. The brain was quickly removed and placed on cold extracellular solution containing (mM): 125 NaCl, 2.5 KCl, 26 $NaHCO_3$, 1.25 NaH_2PO_4, 1 $MgCl_2$, 2 $CaCl_2$ and 10 glucose, pH 7.4 when gassed with 95% O_2–5% CO_2. The cerebellum was dissected and mounted on a modified Oxford vibratome and 300-μm-thick sagittal slices were made. The slices were kept in oxygenated extracellular solution at 34°C for 1 h, and then at room temperature until use.

Extracellular recording

Slices were placed in a recording chamber on the stage of a Zeiss Axioskop microscope. DCN neurons were visually identified using a 40× water-immersion objective with infrared optics. The slices were superfused with the recording solution at a rate of 1.5–2 ml min^{-1} and the temperature adjusted to 35 ± 1°C. To isolate the intrinsic activity of DCN neurons, fast synaptic transmission was blocked using 100 μM picrotoxin (Sigma, St Louis, MO, USA), a $GABA_A$ receptor antagonist (Yoon *et al.* 1993), and 5 mM kynurenic acid (Spectrum Chemical MFG Corp., Gardena, CA, USA), a broad-spectrum ionotropic glutamate receptor antagonist (Stone, 1993).

Extracellular recordings were obtained from single DCN neurons using a home-made differential amplifier and glass pipette electrodes filled with the extracellular solution. Data were sampled at 10 kHz using an analog-to-digital converter (PCI-MIO-16XE-10; National Instruments, Austin, TX, USA), and acquired and analysed using custom software written in LabView (National Instruments). In each experiment, interspike interval histograms were constructed using a long stretch of spontaneous activity (> 5 min). These histograms were used to calculate the predominant (instantaneous) firing rate, defined as the reciprocal of the interspike interval most frequently observed (the peak of the histogram, i.e. its mode), and the maximum (instantaneous) firing rate, defined as the reciprocal of the shortest interspike interval which accounted for at least 5% of interspike intervals (Womack & Khodakhah, 2003).

On average, we obtained a predominant firing rate of 19.9 ± 0.7 spikes s^{-1} ($n = 167$ cells), with a coefficient of variation of the interspike interval of 0.056 ± 0.002. Supplemental Fig. 1*A* shows the histogram of the distribution of firing rates obtained in 167 cells (in the presence of blockers of both excitatory and inhibitory synaptic transmission). The large distribution of the firing rates suggests that all types of DCN neurons were adequately and unbiasedly sampled (Uusisaari *et al.* 2007). Moreover, we did not observe a systematic change in the firing rate of the neurons examined as function of the age of the animals within the range examined (Supplemental Fig. 1*B*; $R^2 = 0.07$ for the linear regression fit to the data).

Apamin was obtained from Sigma. Iberiotoxin, nimodipine and EBIO (1-ethyl-2-benzimidazolinone) were purchased from Tocris (Ellisville, MO, USA). ω-Conotoxin MVIIC and ω-agatoxin IVA were from Bachem (Torrance, CA, USA). ω-Conotoxin GVIA and SNX-482 were from Alomone Laboratories (Jerusalem, Israel). Mibefradil was a generous gift from Hoffmann-La Roche (Basel, Switzerland).

Whole-cell recording

Whole-cell recordings were performed using an Optopatch amplifier (Cairn Research, Kent, UK) with electrodes pulled from borosilicate glass (1–3 MΩ resistance when filled with intracellular solution). The internal solution used for whole-cell current-clamp recordings contained the following (mM): 125 potassium methylsulphate, 10 NaCl, 0.01 EGTA, 9 HEPES, 14 creatine phosphate, 4 MgATP, 0.3 Tris-GTP, and pH 7.2 (KOH). Data were sampled at 20 kHz using an analog-to-digital converter (PCI-MIO-16XE-10; National Instruments), and acquired and analysed using custom software written in LabView (National Instruments). In these experiments action potential threshold was defined as the membrane potential at the foot of an action potential where the rate of rise of potential (the slope) measured between two consecutive data points was at least 5× greater than that in the preceding pair.

The majority of cells recorded in $I = 0$ current-clamp mode were spontaneously active (26 out 29), firing on average at 13.7 ± 1.6 spikes s^{-1}. In three cases, the cells were silent and enough depolarizing current (< 200 pA) was injected to make them fire action potentials.

All data are presented as mean ± S.E.M. Statistical analysis was performed by one-way ANOVA and data were considered not to be statistically different if $P > 0.05$.

Results

Blockade of VGCCs disrupts the spontaneous activity of DCN neurons

Using single cell extracellular recording to avoid alterations in the cytosolic composition of DCN neurons, we examined the contribution of voltage-gated calcium channels (VGCCs) to their spontaneous firing. In order to isolate the intrinsic activity, recordings were performed in the presence of fast synaptic transmission blockers: 5 mM kynurenic acid and 100 μM picrotoxin. We recorded from cells located in the lateral and medial nuclei (15–30 μm soma length). Under control conditions, all cells ($n \approx 170$) showed regular tonic activity and no bursts.

We first applied 100 μM cadmium chloride to block high-threshold VGCCs. Cadmium altered spontaneous activity in one of two ways. In the majority of cells (33 out 44; 75%) cadmium initially increased the predominant firing rate (FR) then caused bursts of action potentials (bursting cells). Figure 1*Aa* shows one example of a bursting cell. In control conditions, the cell fired tonically at ~20 spikes s^{-1}. As cadmium washed in the FR increased and the cell rapidly switched to a bursting mode. The bursting persisted for as long as the activity of the cell was monitored (sometimes in excess of 1 h). In the presence of cadmium, the interspike interval distribution showed a significant leftward shift (Fig. 1*Ab*). On average, both the predominant and maximum FR increased from 18.8 ± 1.2 and 22.3 ± 1.5 spikes s^{-1} under control conditions, to 147.2 ± 18.0 and 292.5 ± 33.6 spikes s^{-1}, respectively, in the presence of cadmium (Fig. 1*Ac*, $P < 0.001$).

In the absence of synaptic inputs, the firing of DCN neurons was extremely regular as evident from the very low (0.06 ± 0.01, $n = 33$) coefficient of variation of interspike interval. As expected from the bursting behaviour, cadmium made the firing quite irregular and the CV increased to 0.59 ± 0.04 ($n = 33$; Fig. 1*Ad*, $P < 0.001$).

In the remainder of the cells (11 out of 44; 25%) cadmium decreased the FR (non-bursting cells). As shown in Fig. 1*Ba* cadmium simply reduced the FR from 18.3 to 9.6 spikes s^{-1} without causing the cell to burst. In the presence of cadmium, the interspike interval distribution shifted to the right and broadened significantly, suggesting that the firing might have become less regular (Fig. 1*Bb*). On average, the predominant FR reduced from 16.3 ± 1.8 to 5.9 ± 1.1 spikes s^{-1} in the presence of cadmium (Fig. 1*Bc*, $P < 0.001$). The maximum FR also decreased from 18.1 ± 2.0 to 10.1 ± 1.5 spikes s^{-1} (Fig. 1*Bc*, maximum FR, $P < 0.01$). As expected from the broader interspike interval distributions, on average the coefficient of variation significantly increased from a control value of 0.04 ± 0.003 to 0.23 ± 0.026 in the presence of cadmium (Fig. 1*Bd*, $n = 11$, $P < 0.001$).

Our results show two markedly different responses following blockade of mainly high-threshold VGCCs in DCN neurons. We wondered whether bursting and non-bursting cells belonged to two separate classes of DCN neurons. It has been recently demonstrated that large non-GABAergic DCN neurons have a higher rate of spontaneous activity (~34 spikes s^{-1}) compared to GABAergic (~12 spikes s^{-1}) and small non-GABAergic cells (~14 spikes s^{-1}) (Uusisaari *et al.* 2007). The scattergram in Fig. 1*Be* shows the effect of cadmium on all 44 cells examined as a function of their baseline spontaneous FR. As can be noted, there was no correlation between the rate of spontaneous activity and whether cadmium caused bursting or whether it decreased the FR. Similarly, there was no correlation between the effect of cadmium and the age of the animal, or the location of the cell (lateral *versus* medial nuclei; data not shown).

Blockade of small-conductance K_{Ca} channels (SK) mimics the action of cadmium on bursting cells

The increase in the FR and the bursting seen after addition of cadmium in the majority of DCN neurons is in agreement with prior suggestions that the net calcium-dependent current is outward (Raman *et al.* 2000). DCN neurons express both large-conductance (BK) and small-conductance (SK) K_{Ca} channels (Chang *et al.* 1997; Sausbier *et al.* 2004; Shakkottai *et al.* 2004). Using specific blockers of these two types of K_{Ca} channels we examined the role that each plays in regulating the spontaneous activity of DCN neurons.

Figure 2*Aa* shows the consequence of application of 100 nM iberiotoxin, a selective BK channel blocker (Galvez *et al.* 1990), in a DCN neuron. As can be noted, iberiotoxin slightly increased the FR from 23.9 to 29.2 spikes s^{-1} without making it irregular. In general, iberiotoxin had a greater effect on the FR of cells that had higher spontaneous FR under control conditions (Fig. 2*Ab*). On average iberiotoxin increased the predominant FR from 20.9 ± 1.9 to 31.1 ± 4.4 spikes s^{-1} and the maximum FR from 25.4 ± 2.5 to 40.4 ± 6.4 spikes s^{-1} (Fig. 2*Ac*, $n = 14$, $P < 0.05$). As stated, iberiotoxin did not significantly change the regularity of the firing; the average coefficient of variation of the interspike interval was 0.05 ± 0.006 under

control conditions, and 0.07 ± 0.012 after application of iberiotoxin (Fig. 2*Ad*).

We next examined the role of SK channels in the regulation of the spontaneous activity of DCN neurons. DCN neurons express SK1, SK2 and SK3 isoforms of SK channels (Bond *et al.* 2000; Sailer *et al.* 2004; Shakkottai *et al.* 2004). As shown in Fig. 2*Ba* application of 100 nM apamin, a selective blocker of SK channels (Blatz &

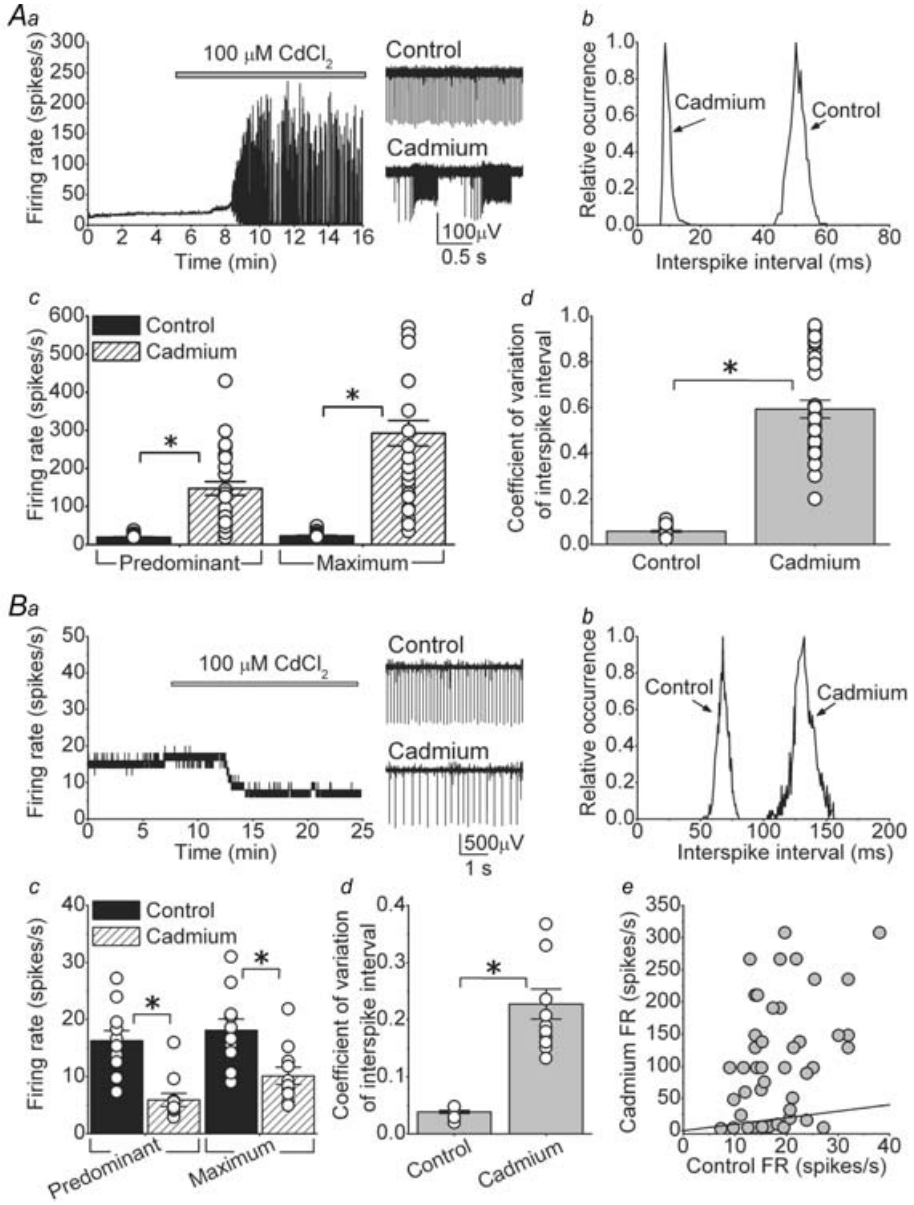

Figure 1. Cadmium-sensitive calcium channels make a significant contribution to the spontaneous activity of the majority of DCN neurons

Spontaneous activity of individual, visually identified DCN neurons was monitored by extracellular recording in acutely prepared slices at 35°C. Fast excitatory and inhibitory synaptic transmission was blocked pharmacologically. *Aa*, application of cadmium increased the firing rate and caused random bursts of action potentials in the majority of DCN neurons. Sample raw data traces are shown in the right panel. *Ab*, interspike interval histogram of the cell shown in *Aa*. *Ac*, predominant and maximum spontaneous firing rates of individual cells together with the averages in the presence and absence of cadmium. $^*P < 0.001$, $n = 33$ cells. *Ad*, the coefficient of variation of the interspike intervals for the same cells shown in *Ac*. $^*P < 0.001$. *Ba*, in a small fraction of cells cadmium simply reduced the firing rate. Sample traces are shown to the right of the panel. *Bb*, interspike interval histogram of the cell shown in *Ba*. *Bc*, predominant and maximum spontaneous firing rates of individual cells together with the averages in the presence and absence of cadmium. $^*P < 0.01$, $n = 11$ cells. *Bd*, the coefficient of variation of the interspike intervals for the same cells shown in *Bc*. $^*P < 0.001$. *Be*, the predominant firing rate of all cells examined (in *A* and *B*) before and after addition of cadmium. The continuous line represents the unity line.

Magleby, 1986), increased the FR and caused bursts of action potentials. Similar effects were seen in 14 out of 19 cells. In contrast to the action of iberiotoxin, there was no relationship between the control FR and the effectiveness of apamin in increasing the FR and causing the cell to burst (Fig. 2*Bb*). In the 14 cells whose activity was affected by apamin, the predominant FR increased from 23.5 ± 3.8 to 165.7 ± 27.8 spikes s^{-1} after apamin (Fig. 2*Bc*, $P < 0.001$). The maximum FR also increased from 28.6 ± 4.9 to 316.7 ± 46.2 spikes s^{-1}

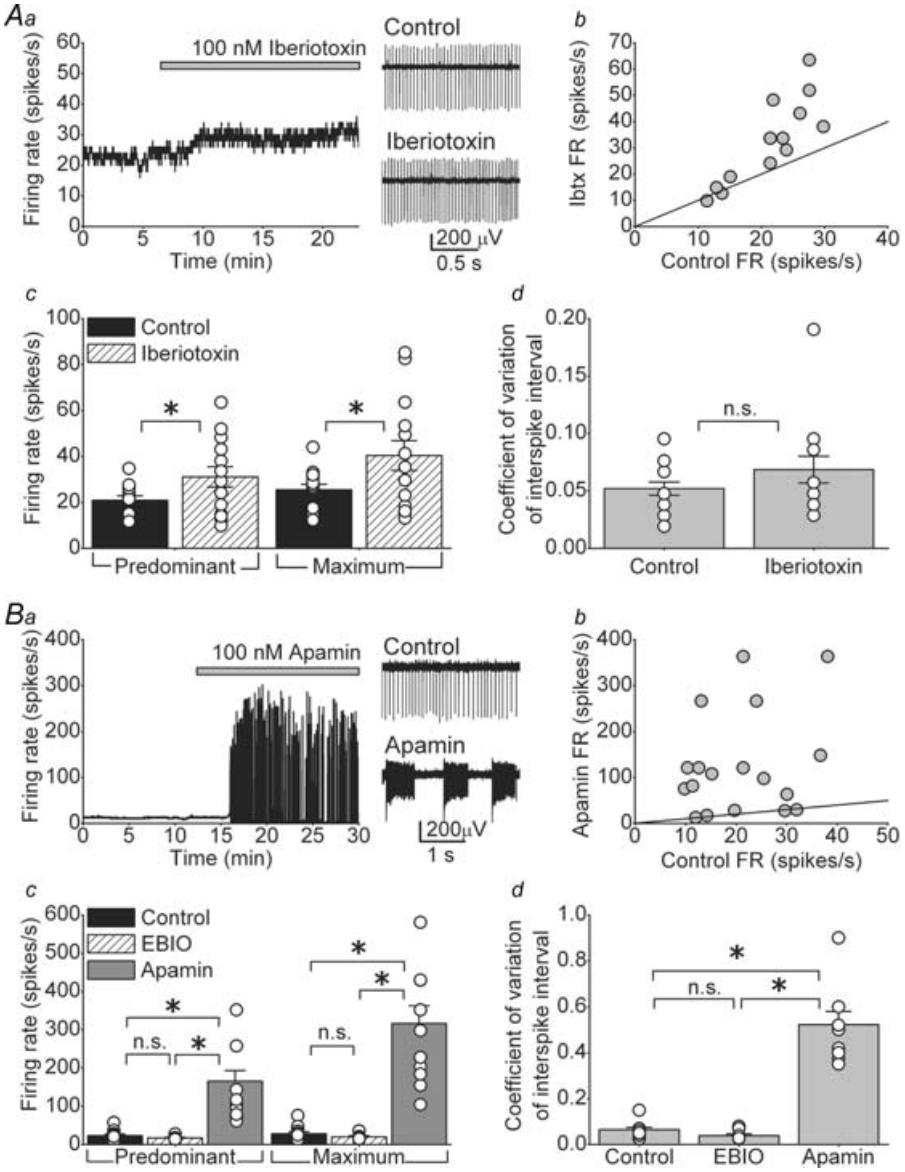

Figure 2. K_{Ca} channels, particularly of the SK type, control the rate of intrinsic activity of DCN neurons
Aa, the spontaneous activity of a DCN neuron as large-conductance K_{Ca} (BK) channels were blocked with 100 nM iberiotoxin. *Ab*, the firing rate of DCN neurons before (control) and after application of iberiotoxin. The continuous line denotes unity. *Ac*, predominant and maximum spontaneous firing rates of individual cells together with the averages in the presence and absence of iberiotoxin. $^*P < 0.05$, $n = 14$ cells. *Ad*, the coefficient of variation of the interspike intervals for the same cells shown in *Ac*. *Ba*, blockade of small-conductance (SK) K_{Ca} channels with 100 nM apamin increased the firing rate and resulted in high-frequency bursts of action potentials. *Bb*, the firing rate of DCN neurons before (control) and after application of apamin. The continuous line denotes unity. *Bc*, predominant and maximum spontaneous firing rates of individual cells together with the averages in the presence and absence of 20 μM EBIO ($n = 7$) or 100 nM apamin ($n = 14$). $^*P < 0.001$. *Bd*, the coefficient of variation of the interspike intervals for the same cells shown in *Bc*. $^*P < 0.001$. n.s., not significant.

(Fig. 2*Bc*, $P < 0.001$). Consistent with the bursting, the coefficient of variation of the interspike intervals markedly increased after application of apamin from 0.06 ± 0.01 to 0.52 ± 0.06 (Fig. 2*Bd*, $P < 0.001$). The effect of apamin on the FR was quantitatively comparable to the action of cadmium, suggesting that the bulk of K_{Ca} channels that regulate the spontaneous activity of DCN neurons are of the SK type (Aizenman & Linden, 1999).

In 5 out of the 19 cells examined we did not observe any effect of apamin on the predominant FR (21.5 ± 4.0 spikes s^{-1} in control *versus* 23.1 ± 3.4 spikes s^{-1} after apamin application), the maximum FR (25.1 ± 4.9 spikes s^{-1} in control, compared to 30.9 ± 4.6 spikes s^{-1} after apamin application) or the coefficient of variation of the interspike interval (0.07 ± 0.006 in control and after apamin application) (data not shown).

Similar to that seen here for DCN neurons, SK channels also regulate the firing rate and regularity of pacemaking in Purkinje cells (Womack & Khodakhah, 2003; Walter *et al.* 2006). A small reduction in the calcium current density in Purkinje cells, whether as a consequence of a genetic defect in P/Q-type calcium channels or their pharmacological blockade, decreases the precision of pacemaking whereas larger reductions in the current density cause avid bursting (Womack & Khodakhah, 2003; Walter *et al.* 2006). It has been recently demonstrated that low concentrations (10–20 μM) of the pharmacological activator of SK channels, EBIO (Pedarzani *et al.* 2001), rescues the irregular FR observed in Purkinje cells of P/Q-type channel ataxic mice and, when chronically perfused into the cerebellum, reduces ataxia (Walter *et al.* 2006). These perfusion studies did not restrict diffusion of EBIO solely to the cerebellar cortex and it is likely that the DCN neurons were also exposed to EBIO. Thus, it is possible that actions of EBIO, in part, may have been mediated by alterations in the activity of DCN neurons. To investigate such a possibility we examined whether comparable concentrations of EBIO that affect firing of Purkinje cells also affect the FR of DCN neurons. In none of the seven DCN neurons examined, however, did 20 μM EBIO alter either the FR or the regularity of pacemaking (Fig. 2*Bc*, control predominant FR $= 17.6 \pm 2.1$ *versus* 17.2 ± 2.3 spikes s^{-1} in EBIO; control maximum FR $= 20.6 \pm 3.0$ *versus* 20.1 ± 3.4 spikes s^{-1} in EBIO, $P = 0.9$ for both). In 20 μM EBIO, the coefficient of variation of interspike intervals was also not significantly different from the control condition (Fig. 2*Bd*, CV in control $= 0.05 \pm 0.01$ compared to CV in EBIO $= 0.04 \pm 0.01$, $n = 7$ cells, $P = 0.41$). A small (~20%) but statistically significant decrease in the firing rate was only observed when the EBIO concentration was increased to 100 μM (Supplemental Fig. 2*A*). At these higher concentrations, there was also a notable reduction in the coefficient of variation of interspike intervals (Supplemental Fig. 2*B*).

To ensure that the effects of EBIO were mediated via SK channels, in 10 cells we measured the FR and coefficient of variation of the interspike interval when 100 μM EBIO was perfused after 100 nM apamin. With SK channels blocked, EBIO did not alter the FR or the coefficient of variation (predominant FR $= 165.5 \pm 18.2$ spikes s^{-1}, maximum FR $= 268.9 \pm 23.6$ spikes s^{-1} ($P = 0.98$ for predominant FR and $P = 0.15$ for maximum FR *versus* apamin alone), and the coefficient of variation of interspike interval $= 0.66 \pm 0.09$, $P = 0.82$ *versus* apamin alone), confirming that its actions were selectively mediated by SK channels.

L, P/Q-, R- and T-type VGCCs do not regulate the spontaneous activity of DCN neurons

The preceding data demonstrate that in the majority of DCN neurons calcium influx via cadmium-sensitive calcium channels activates SK channels that regulate their spontaneous firing. In several neurons, specific VGCCs are selectively coupled with K_{Ca} channels. For example, in cerebellar Purkinje cells K_{Ca} channels are selectively activated by calcium influx through P/Q-type calcium channels (Womack *et al.* 2004) whereas in midbrain dopaminergic neurons, this role is performed by T-type calcium channels (Wolfart & Roeper, 2002). Immunohistochemical studies have shown the expression of several pore-forming α subunits of VGCCs in the cerebellar nuclei, including: α_{1A} (P/Q-type), α_{1B} (N-type), α_{1C} and α_{1D} (L-type) (Chung *et al.* 2000), and α_{1E} (R-type) (Volsen *et al.* 1995). T-type isoforms α_{1G}, α_{1H} and α_{1I} are also expressed in different populations of DCN neurons (Molineux *et al.* 2006). Therefore, at the protein level, DCN neurons express all types of VGCCs.

We used selective pharmacological blockers of different VGCCs to identify those that are coupled to the activation of K_{Ca} channels. Figure 3*Aa* shows an example of a cell to which a combination of blockers of L-, P/Q- and R/T-type calcium channels was applied. As can be seen, concurrent bath perfusion of 2 μM nimodipine, an L-type channel blocker (Fanelli *et al.* 1994), 200 nM ω-agatoxin IVA, a P/Q-type channel blocker (Mintz *et al.* 1992), and 5 μM mibefradil which blocks most R- and T-type channels (Martin *et al.* 2000; McDonough & Bean, 1998), did not significantly affect the activity of the cell, although a very small leftward shift in the interspike interval distribution can be noted in this cell (Fig. 3*Ab*). Similar data were also obtained when 100 nM SNX-482 was added to specifically block R-type channels (Newcomb *et al.* 1998). On average, as shown in Fig. 3*B*, in 50 cells where blockers of L-, P/Q- and R/T-type channels were applied separately or as a mixture together, the predominant and maximum FRs were not significantly different from those under control conditions (predominant FR $= 20.6 \pm 1.5$ spikes s^{-1} in

control, and 21.0 ± 1.6 spikes s^{-1} after the application of blockers; maximum FR in control $= 24.1 \pm 1.8$ spikes s^{-1}, after blockers $= 25.5 \pm 2.0$ spikes s^{-1}, $P = 0.84$ for predominant and $P = 0.6$ for maximum). Similarly, block of L-, P/Q- and R/T-type calcium channels did not affect the regularity of the FR as evident from the comparable coefficients of variation of interspike intervals before and after application of all blockers ($CV = 0.06 \pm 0.004$ in control and 0.07 ± 0.006 in blockers, Fig. 3*C*, $P = 0.17$). The lack of effectiveness of these blockers in altering the FR was independent of the FR in control conditions (Fig. 3*D*). As a control for the effectiveness of ω-agatoxin IVA we recorded the activity of several Purkinje cells in the same slices in which it did not affect the firing rate of DCN neurons. In every case examined, consistent with prior published work (Womack & Khodakhah, 2002), we found that ω-agatoxin IVA had increased the firing rate of Purkinje cells such that they were bursting at very high rates (data not shown).

N-type calcium channels make a significant contribution to the intrinsic firing of DCN neurons

On the basis of the data presented in the earlier section, we expected that blockade of N-type calcium channels should have a significant effect on the spontaneous activity of DCN neurons. Indeed, as shown in Fig. 4*Aa*, addition of 1 μM ω-conotoxin GVIA (Cgtx GVIA, a selective N-type blocker) (Reynolds *et al.* 1986; McCleskey *et al.* 1987), to a mixture of L-, P/Q- and R/T-type calcium channels blockers significantly increased the FR and caused the cell to burst. The increase in the FR after blockade of N-type calcium channels is evident in the interspike interval distribution shown in Fig. 4*Ab* in which the combination of blockers did not affect the interspike interval distribution but adding the N-type blocker caused a major leftward shift. Comparable results were obtained when instead of Cgtx GVIA we used 1 μM ω-conotoxin MVIIC (Cgtx MVIIC (Stocker *et al.* 1997). Addition of one N-type blocker to the mixture of L-, P/Q- and R/T-type blockers increased the FR and caused bursting in 22 out of 28 cells examined. In these 22 cells the predominant FR increased from an average of 23.4 ± 3.8 to 84.9 ± 12.6 spikes s^{-1}. Similarly, the maximum FR increased from 27.6 ± 4.5 to 164.3 ± 26.0 spikes s^{-1} (Fig. 4*Ac*; $P < 0.001$, $n = 22$ cells). Because of the bursting, the coefficient of variation of interspike intervals increased from 0.07 ± 0.01 in the presence of L-, P/Q- and R/T-type blockers, to 0.44 ± 0.05 after adding the N-type blocker (Fig. 4*Ad*; $P < 0.001$).

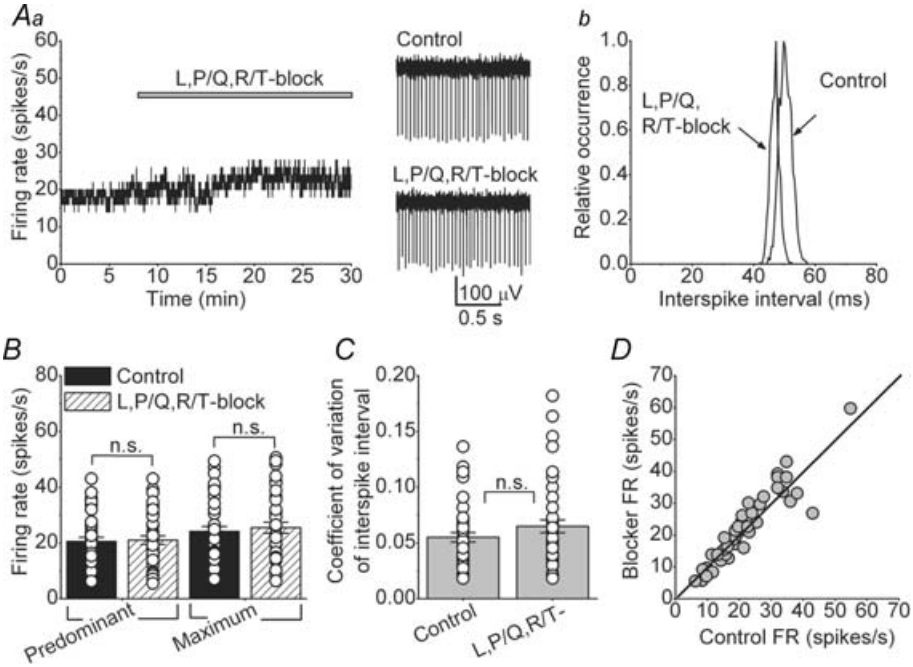

Figure 3. L-, P/Q- and R/T-type voltage-gated calcium channels do not contribute to the spontaneous activity of DCN neurons

A, bath application of a combination of L-, P/Q- and R/T-calcium channels blockers (2 μM nimodipine, 200 nM ω-agatoxin IVA and 5 μM mibefradil, respectively) did not significantly alter the spontaneous activity of a DCN neuron. *Ab*, interspike interval histogram of the cell shown in *A*. *B*, predominant and maximum spontaneous firing rates of individual cells together with the averages in the presence and absence of a combination of L-, R/T- and P/Q-type calcium channel blockers. $n = 50$ cells. *C*, the coefficient of variation of the interspike intervals for the same cells shown in *B*. *D*, the firing rate of all cells examined before and after addition of L-, R/T- and P/Q-type calcium channel blockers. The continuous line represents the unity line. n.s., not significant.

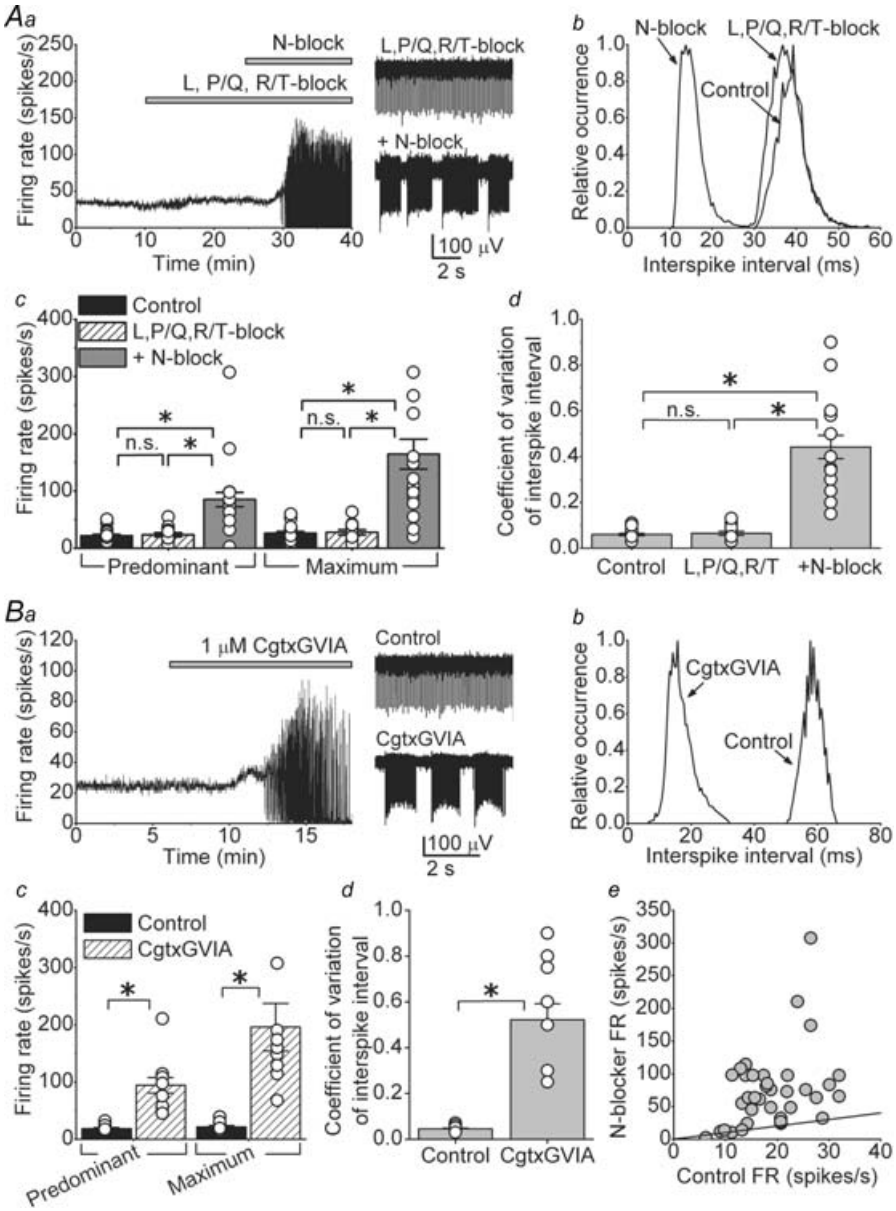

Figure 4. Block of N-type calcium channels increases the firing rate and causes bursting in the majority of DCN neurons

Aa, the rate of spontaneous activity of a DCN neuron in control solution and after sequential addition of a mixture of L-, P/Q- and R/T-type calcium channel blockers (2 μM nimodipine, 200 nM ω-agatoxin IVA and 5 μM mibefradil) and 1 μM ω-conotoxin (Cgtx) GVIA to block N-type calcium channels. Representative raw data traces are also shown. *Ab*, interspike interval histogram of the cell shown in *Aa*. *Ac*, predominant and maximum spontaneous firing rates of individual cells together with the averages in the presence and absence of the mixture of L-, P/Q- and R/T-type calcium channel blockers, and after the subsequent addition of a N-type calcium channel blocker (either 1 μM Cgtx GVIA or 1 μM Cgtx MVIIC). $^*P < 0.001$; n.s., not significant, $n = 22$ cells. *Ad*, the coefficient of variation of the interspike intervals for the same cells shown in *Ac*. $^*P < 0.001$; n.s., not significant. *Ba*, application of 1 μM Cgtx GVIA to block N-type calcium channels in the absence of any other calcium channel blocker also increased the firing rate and caused the cell to burst. *Bb*, interspike interval histogram of the cell shown in *Ba*. *Bc*, predominant and maximum spontaneous firing rates of individual cells together with the averages in the presence and absence of Cgtx GVIA. $^*P < 0.001$, $n = 14$ cells. *Bd*, the coefficient of variation of the interspike intervals for the same cells shown in *Bc*. $^*P < 0.001$. *Be*, the firing rate of all cells examined (in *A* and *B*) before and after the addition of the N-type calcium channel blocker. The continuous line represents the unity line.

In 6 out of 28 cells, addition of N-type blocker to the combination of L-, P/Q- and R/T-type blockers did not cause a major change in FR (predominant FR = 13.9 ± 2.8 in the presence of L-, P/Q- and R/T-type blockers, and 21.9 ± 4.3 spikes s^{-1} after the addition of the N-type channel blocker, data not shown).

Blockade of L-, P/Q- and R/T-type calcium channels was not a prerequisite for the effects of N-type channel blockade on the spontaneous firing of DCN neurons. As can be seen in Fig. 4*Ba*, application of 1 μM Cgtx GVIA alone increased the FR and caused bursts of action potentials (Fig. 4*Ba* and *Bb*). Similar results were obtained in 14 out of 19 cells to which 1 μM Cgtx GVIA was added. In the 14 cells where blockade of N-type channels altered the FR, the average predominant FR increased from 18.3 ± 1.9 to 91.3 ± 10.7 spikes s^{-1}, and the average maximum FR increased from 21.0 ± 2.3 to 194.8 ± 34.1 spikes s^{-1} (Fig. 4*Bc*, $P < 0.001$). Similarly the coefficient of variation of interspike intervals increased from 0.05 ± 0.003 to 0.52 ± 0.07 (Fig. 4*Bd*, $P < 0.001$). There was no correlation between the basal activity of the cell and whether the N-type channel blocker caused the cell to burst or not (Fig. 4*Be*, including all 47 cells shown in *A* and *B*).

In the five cells where application of Cgtx GVIA did not cause bursting, neither the predominant FR nor the maximum FR significantly changed (predominant FR = 17.6 ± 3.2 spikes s^{-1} in control and 25.6 ± 4.7 spikes s^{-1} after Cgtx GVIA; maximum FR = 22.5 ± 3.9 spikes s^{-1} in control and 34.6 ± 6.2 spikes s^{-1} after Cgtx GVIA; coefficient of variation in control = 0.1 ± 0.02 and after Cgtx GVIA = 0.15 ± 0.01).

Additional cadmium-sensitive calcium-permeable channels may be present in DCN neurons

Our pharmacological analysis of the role of various VGCCs in DCN neurons suggests that N-type but not L-, P/Q- or R/T-type calcium channels significantly contribute to the spontaneous activity in these neurons. Blockade of N-type calcium channels increased the FR and caused cells to burst, consistent with the notion that they are coupled to K_{Ca} channels, and that the net calcium-dependent current is outward. Although the bursting seen following selective block of N-type calcium channels is reminiscent of blockade of SK channels with apamin and calcium influx by cadmium, there are quantitative differences. For example, the maximum FR achieved in the presence of the cocktail of blockers of high-threshold VGCCs (including N-type channels; Fig. 4*Ac*) is significantly lower than that in the presence of cadmium (Fig. 1*Ac*) or apamin (Fig. 2*Bc*). Indeed, as can be seen in Fig. 5*A*, application of 100 nM apamin after blocking all VGCCs (L-, N-, P/Q- and R/T-type) with the toxins described earlier significantly increased the predominant FR from 74.7 ± 6.9 to 164.6 ± 29.4 spikes s^{-1} (Fig. 5*A*, $n = 8$ cells) and reduced the duration of the bursts from 0.99 ± 0.27 to 0.61 ± 0.0.1 s (data not shown). It is probable that cadmium blocks additional calcium influx pathways to those blocked by the specific toxins we used, and that this additional calcium flux is coupled to the activation of SK channels. Alternatively, it may be that at the concentrations used, the toxins had not completely blocked all the targeted calcium channels. We explored this latter possibility further as detailed below.

Given that SNX-482 blocks different isoforms of the R-type channel with different affinities, some requiring relatively high concentrations (Tottene *et al.* 2000), we tested the efficacy of 500 nM SNX-482 in increasing the FR of DCN neurons when L-, N-, P/Q- and R/T-type calcium channels were already blocked by a mixture of 2 μM nimodipine, 1 μM Cgtx GVIA, 200 nM ω-agatoxin IVA and 5 μM mibefradil (Fig. 5*B*). As can be noted in Fig. 5*Ba* and *Bb*, even 500 nM SNX-482 did not increase the FR or affected the bursts. In the nine cells examined, the predominant and maximum FR in the presence of the mixture of L-, N-, P/Q- and R/T-type calcium channels blockers were 82.7 ± 17.9 and 195.6 ± 41.1 spikes s^{-1}, respectively, and after adding 500 nM SNX-482 they were 82.3 ± 17.7 and 197.8 ± 41.9 spikes s^{-1} (Fig. 5*Ac*, $P = 0.99$ for both FR). Thus, we conclude that R-type calcium channels do not contribute to the spontaneous activity in DCN neurons.

We next considered the possibility that we have not blocked all N-type calcium channels using 1 μM Cgtx MVIIC or GVIA, even though it is known that within the physiologically relevant range of membrane potentials, the affinities of these toxins for N-type channels are in the nanomolar range (Boland *et al.* 1994). We used both toxins together each at the higher concentration of 3 μM. Figure 5*Ca* shows an example of a cell treated with a mixture of 3 μM Cgtx MVIIC and 3 μM Cgtx GVIA. As can be seen in Fig. 5*Ca* and the associated histograms in Fig. 5*Cb*, the increase in the FR and the bursts at these higher toxins concentrations were comparable to those obtained using 1 μM of each toxin. On average, the predominant and maximum FR in control were 17.3 ± 0.9 and 19.7 ± 1.2 spikes s^{-1}, respectively, and increased to 76.8 ± 11.1 and 173.8 ± 21.2 spikes s^{-1} after addition of both toxins (Fig. 5*Cb*, $P < 0.001$, $n = 17$). These values were not statistically different from the values obtained with 1 μM Cgtx GVIA alone ($P = 0.36$ for predominant FR and $P = 0.5$ for maximum FR). The duration of the bursts was also equivalent under both toxin concentrations (burst duration in Cgtx GVIA at 1 μM = 1.36 ± 0.17 s *versus* 1.25 ± 0.29 s in Cgtx MVIIC and GVIA at 3 μM each, $P = 0.7$)

To confirm the existence of a calcium influx pathway additional to N-type calcium channels, we applied 100 μM

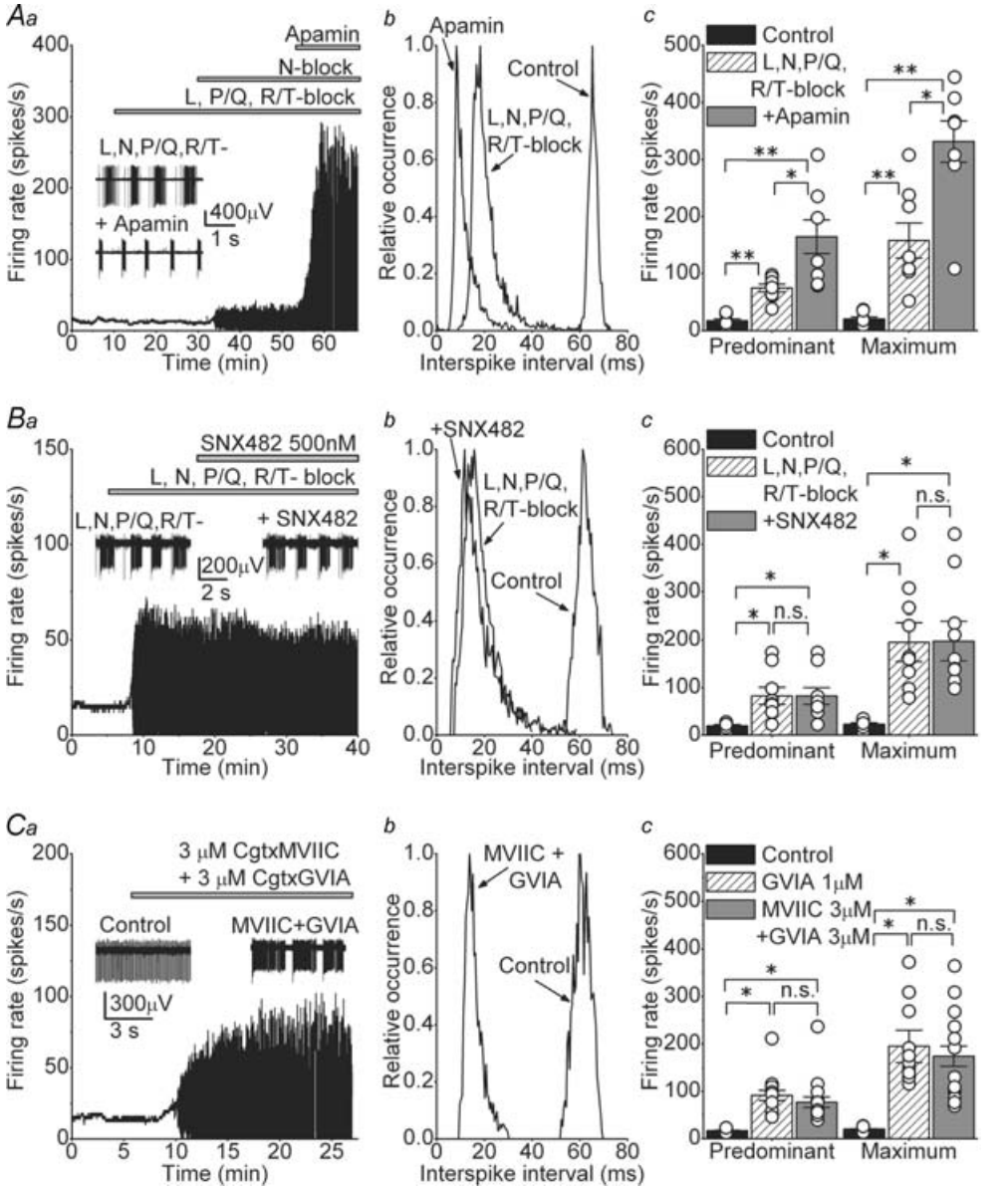

Figure 5. Additional calcium influx pathways activate SK channels and contribute to the firing rate of DCN neurons

Aa, the rate of spontaneous activity of a DCN neuron in control solution and after sequential addition of a mixture of L-, P/Q- and R/T-type calcium channel blockers (2 μM nimodipine, 200 nM ω-agatoxin IVA and 5 μM mibefradil), then 1 μM Cgtx GVIA to block N-type calcium channels, and 100 nM apamin to block SK channels. The inset shows raw traces before and after application of apamin. *Ab*, interspike interval histogram of the cell shown in *Aa*. *Ac*, predominant and maximum spontaneous firing rates of individual cells together with the averages in control, after L-, N-, P/Q- and R/T-type calcium channels were blocked by 2 μM nimodipine, 1 μM Cgtx GVIA, 200 nM ω-agatoxin IVA and 5 μM mibefradil (L-, N-, P/Q- and R/T-block), and after the successive addition of 100 nM apamin. $^*P < 0.01$ in predominant FR and $P < 0.05$ in maximum FR. $^{**}P < 0.001$, $n = 8$ cells. *Ba*, the rate of spontaneous activity of a DCN neuron in control solution and after sequential addition of L-, N-, P/Q- and R/T-type calcium channels blockers, and 500 nM SNX-482 to specifically block R-type calcium channels. The inset shows example of raw traces obtained before and after addition of SNX-482. *Bb*, histogram of the interspike interval distribution of the cell in *Ba*. *Bc*, individual and average firing rates obtained in 9 cells in control, after blocking L-, N-, P/Q- and R/T-type calcium channels and after blocking all R-type channels with SNX-482 $^*P < 0.001$. *Ca*, continuous recording of a cell in control conditions and after adding a combination of Cgtx MVIIC and Cgtx GVIA both at 3 μM. The inset shows example of raw data showing the bursts observed after the toxins. *Cb*, distribution of interspike intervals before and after concurrent addition of 3 μM Cgtx MVIIC and 3 μM Cgtx GVIA. *Cc*, average and individual data from the cells exposed to the combination of toxins before and after. The FR obtained in the presence of 1 μM Cgtx GVIA is also plotted to allow direct comparison. $^*P < 0.001$; n.s., not significant, $n = 17$.

cadmium chloride to the cells treated with both toxins Cgtx MVIIC and GVIA at 3 μM each (Fig. 6*A*). As observed in Fig. 6*Aa* and *Ab*, cadmium further increased the FR and also reduced the duration of the bursts. On average the predominant and maximum FR in the presence of both Cgtx MVIIC and GVIA at 3 μM were 81.6 ± 12.6 and 154.6 ± 36.9 spikes s^{-1}, respectively; after adding cadmium they increased to 165.9 ± 30.1 and 293.2 ± 60.5 spikes s^{-1} ($P < 0.01$ for predominant and $P < 0.05$ for maximum FR, $n = 11$). Cadmium also reduced the duration of the bursts as observed in the right panels in Fig. 6*Aa*. Figure 6*B* shows summary data from nine cells where 50 μM nickel chloride and then 100 μM cadmium chloride were sequentially added to cells previously exposed to 2 μM nimodipine, 1 μM Cgtx GVIA, 200 nM ω-agatoxin, 500 nM SNX-482 and 5 μM mibefradil to block L-, N-, P/Q-, R- and T-type calcium channels, respectively. While neither 500 nM

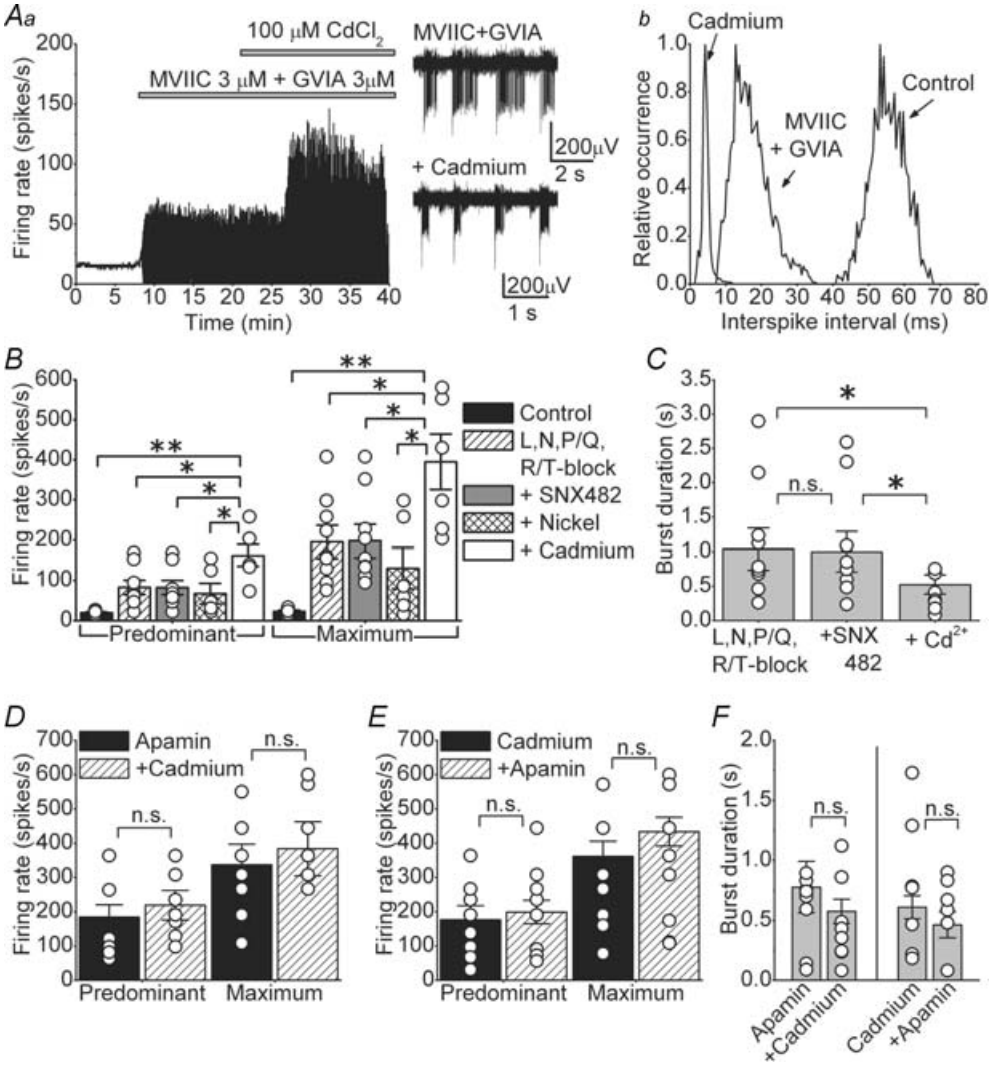

Figure 6. Blockade of calcium influx with cadmium has comparable effects as block of SK channels with apamin

Aa, application of 100 μM cadmium after concurrent application of Cgtx MVIIC and GVIA both at 3 μM further increased the firing rate and reduced the duration of the bursts. Sample raw data are also shown. *Ab*, histogram of the interspike interval of the cell in *Aa*. *B*, average and individual data obtained after sequentially adding: a mixture of blockers of L-, N-, P/Q- and R/T-type calcium channels (2 μM nimodipine, 1 μM Cgtx GVIA, 200 nM ω-agatoxin and 5 μM mibefradil), then 500 nM SNX-482 (to block R-type calcium channels), then 50 μM nickel and finally 100 μM cadmium. $^*P < 0.05$, $^{**}P < 0.001$, $n = 9$ cells. *C*, average and individual data showing the duration of the bursts for the same cells presented in Fig. 6*B*. $^*P < 0.05$. *D*, average and individual firing rates in cells first exposed to 100 nM apamin and then to 100 μM cadmium. *E*, average and individual firing rates in cells first exposed to 100 μM cadmium and then to 100 nM apamin. *F*, average and individual data showing the duration of the bursts for the same cells presented in *D* and *E*. n.s., not significant.

SNX-482 nor 50 μM nickel (which at these concentrations should block most R-type calcium channels; Tottene *et al.* 2000) significantly altered the FR, addition of cadmium further increased the FR of each cell tested. In all cases, cadmium also significantly reduced the duration of bursts (Fig. 6*C*). On average the burst duration in L-, N-, P/Q- and R/T-type calcium channels blockers was 1.03 ± 0.31 s, burst duration after adding 500 nM SNX-482 was 0.98 ± 0.29 s ($P = 0.92$ *versus* all other blockers), and the burst duration after addition of cadmium was 0.53 ± 0.14 s ($P < 0.05$ *versus* both previous conditions).

We next sought to ascertain that cadmium increases the FR by blocking a calcium conductance coupled to SK channels. To do so, we first blocked SK channels with 100 nM apamin and then applied 100 μM cadmium. Application of cadmium after apamin did not significantly alter either the predominant or the maximum FR in the nine cells examined (Fig. 6*D*, $P = 0.36$ for predominant and $P = 0.1$ for maximum FR). Similarly, in reciprocal experiments, application of apamin after cadmium did not affect the FR in the eight cells tested (Fig. 6*E*, $P = 0.54$ for predominant and $P = 0.65$ for maximum FR). In none of these experiments did secondary application of cadmium or apamin alter the duration of the bursts (Fig. 6*F*, $P = 0.33$ for burst duration obtained with application of apamin after cadmium; $P = 0.41$ for burst duration in the reciprocal experiment).

Collectively the data presented in this section point toward the presence of a cadmium-sensitive calcium conductance which is coupled to the activation of SK channels, but is pharmacologically distinct from L-, N-, P/Q- and R/T-type calcium channels.

N-type calcium channels contribute to the afterhyperpolarization in DCN neurons

DCN neurons have a prominent afterhyperpolarization (AHP), which is mainly regulated by K_{Ca} channels (Raman *et al.* 2000; Czubayko *et al.* 2001; Shakkottai *et al.* 2004). Given that only N-type calcium channels regulate the spontaneous activity of DCN neurons by activating K_{Ca} channels, it is predicted that blocking N-type calcium channels should reduce the AHP amplitude. To address this question, we recorded spontaneous action potentials in whole-cell current-clamp mode in DCN neurons (Fig. 7*A*). Application of L-, P/Q- and R/T-type channels blockers did not affect either the action potential threshold or the maximum AHP amplitude in any of the 12 cells examined (Fig. 7*Aa–c*). In contrast, application of 1 μM Cgtx GVIA after L-, P/Q- and R/T-type blockers significantly reduced the AHP amplitude in all six cells examined (Fig. 7*Ac*, control $= -62.7 \pm 1.7$ mV; L-, P/Q- and R/T-type blockers $= -64.8 \pm 1.7$ mV; after addition of Cgtx GVIA $= -56.1 \pm 1.4$ mV; $^{*}P < 0.03$, $^{**}P < 0.005$), without altering the action potential threshold (Fig. 7*Ab*, control $= -40 \pm 1.8$ mV; L-, P/Q- and R/T-type blockers $= -39.9 \pm 2.3$ mV; after addition of Cgtx GVIA $= -38.5 \pm 2.7$ mV).

The whole-cell current-clamp data presented are in agreement with predictions made on the basis of extracellular recording. Namely, only blockade of N-type calcium channels, and not L-, P/Q- or R/T-type channels, reduced the AHP amplitude. Surprisingly, in contrast to the data obtained with extracellular recording, in none of the cells examined with whole-cell recording did block of N-type calcium channels increase the FR (control $= 11.1 \pm 1.6$ spikes s^{-1}; L-, P/Q- and R/T-type channel blockers $= 11.1 \pm 2.1$ spikes s^{-1}; after adding Cgtx GVIA $= 10 \pm 2.6$ spikes s^{-1}). The lack of an effect of the VGCCs blockers on the FR of cells recorded in the whole-cell configuration is consistent with the observation made by Raman and colleagues (Raman *et al.* 2000) that block of SK channels also did not increase the FR although it reduced the AHP amplitude (but see also Czubayko *et al.* 2001). It is conceivable that the difference between the data obtained with whole-cell recordings and those with extracellular recording is because of dialysis of the intracellular milieu and alterations in calcium buffering that can occur with whole-cell recordings. In particular, in these experiments the N-type calcium channel blocker was applied more than 30 min after achieving whole-cell configuration. This is because we first obtained 10 min of baseline FR and then applied the mixture of L-, P/Q- and R/T-type channels blockers for at least 20 min before applying the N-type channel blocker.

We investigated whether preventing extended dialysis of the cell would unmask an increase in FR when N-type calcium channels are blocked. Thus, we applied Cgtx GVIA soon after establishing whole-cell configuration (typically in < 5 min). Figure 7*B* shows the FR of a cell before and after 1 μM Cgtx GVIA. As can be seen, block of N-type channels in the absence of extensive dialysis of the cell increased the FR and caused the cell to burst. Similarly, application of 100 μM cadmium soon after going whole-cell increased the FR and caused bursting (Fig. 7*C*). Selective block of N-type calcium channels or all calcium influx by cadmium decreased the AHP, and as expected cadmium did so to a greater extent although the difference was not statistically different (Fig. 7*D*, AHP in control $= -60.2 \pm 16$ mV and after Cgtx GVIA $= -54.6 \pm 2.2$ mV, $P < 0.05$, $n = 7$; AHP in cadmium $= -50.2 \pm 2.3$ mV *versus* -58.2 ± 2.4 mV in control, $P < 0.05$, $n = 6$; $P = 0.19$ AHP in Cgtx GVIA *versus* AHP in cadmium). Also, consistent with that seen with extracellular recordings, cadmium was more effective in increasing the FR than was block of N-type calcium channels with Cgtx GVIA (Fig. 7*E*). On average, the FR in control was 14.6 ± 3.3 spikes s^{-1} and after Cgtx GVIA increased to 31.6 ± 7.4 spikes s^{-1} ($P < 0.05$, $n = 7$); after

cadmium the FR increased to 59.7 ± 9.6 spikes s^{-1} from a control of 16.9 ± 5.2 spikes s^{-1} ($n = 6$, $P < 0.05$ *versus* control and *versus* Cgtx GVIA). However, it is noteworthy that the increases in the FR seen with whole-cell recordings were less than those seen with extracellular recordings, suggesting that even dialysis of the cell for a few minutes altered its excitability.

Discussion

Here we show in juvenile rats that SK channels efficiently regulate the rate of spontaneous activity of most DCN neurons, and demonstrate that the major source for their activation is calcium influx via N-type calcium channels. Thus, although at the protein level DCN neurons express

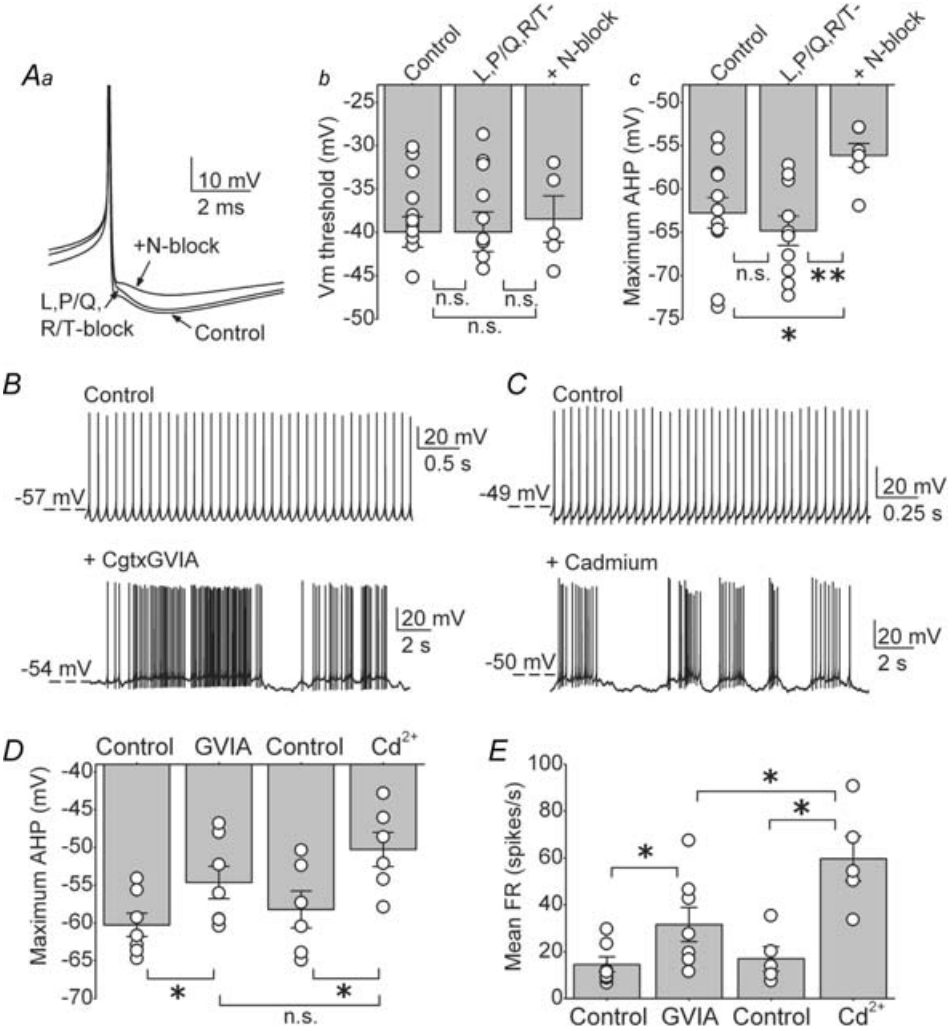

Figure 7. N-type, but not L-, P/Q- or R/T-type, calcium channels significantly contribute to the action potential afterhyperpolarization in DCN neurons

Aa, truncated traces of action potentials obtained from whole-cell current clamp recording from a DCN neuron in $I = 0$ mode before (control), and after sequential additions of a mixture of L-, P/Q- and R/T-type calcium channel blockers (2 μM nimodipine, 200 nM ω-agatoxin IVA and 5 μM mibefradil) and 1 μM Cgtx GVIA to block N-type calcium channels. *Ab*, the action potential threshold of individual cells together with the averages in control solution, in the presence of a mixture of L-, P/Q- and R/T-type calcium channel blockers (2 μM nimodipine, 200 nM ω-agatoxin IVA and 5 μM mibefradil), and subsequent block of N-type calcium channels with 1 μM Cgtx GVIA. *Ac*, the average maximum afterhyperpolarization (AHP) and individual data for the same cells and conditions shown in *B*. $^*P < 0.03$, $^{**}P < 0.005$. $n = 12$ cells for control and L-, P/Q- and R/T-type calcium channels, $n = 6$ after addition of N-type blocker. *B*, raw traces of whole-cell current clamp recordings in control conditions and after adding 1 μM Cgtx GVIA. *C*, similar to *B*; current clamp recordings before and after application of 100 μM cadmium. *D*, maximum AHP of the action potential waveform measured in the cells recorded soon after establishing whole-cell configuration (*B* and *C*). Average and individual data are plotted per condition. $^*P < 0.01$. $n = 7$ cells in Cgtx GVIA and $n = 6$ cells in cadmium. *E*, mean firing rate of the same cells in *D*. The graph shows the average and the individual values obtained in each condition. $^*P < 0.05$. n.s., not significant.

almost all calcium channel types, only the N-type calcium channels seems to regulate pacemaking in DCN neurons.

The function of voltage-gated calcium channels in DCN neurons

We found that blockade of VGCCs disrupts the normal tonic activity in the majority of juvenile DCN neurons (∼75%) causing random high-frequency bursts of action potentials. Clearly in these cells the net calcium-dependent current is outward (Raman *et al.* 2000). In a relatively small population of DCN neurons, blockade of VGCCs reduced the firing rate. This suggests that, similar to for example dopaminergic neurons of the midbrain (Puopolo *et al.* 2007) and neurons of the main olfactory bulb (Puopolo *et al.* 2005), the calcium current contributes a net inward current. On the basis of the baseline firing rate of the cells examined we did not find any evidence that the two types of response belonged to separate classes of neurons, nor that there were any signs of age dependence. However, we cannot rule out the possibility that a rigorous immunohistochemical examination might not reveal the presence of different populations. Moreover, we cannot rule out that the properties of adult DCN neurons may be different given that it has been shown that the expression of calcium channels changes throughout the brain as the animals mature (Tanaka *et al.* 1995).

Comparable to the differential effects of cadmium, we find that blockade of SK channels with apamin affected the intrinsic activity of most, but not all, DCN neurons of juvenile rats. Our data are in agreement with those of Czubayko and colleagues who reported that apamin changed the AHP (and significantly increased the firing rate) in the majority of DCN cells tested, whereas in a small group of cells apamin did not affect the AHP and only slightly increased the firing rate (Czubayko *et al.* 2001).

Selective functional coupling between SK channels and N-type voltage-gated calcium channels in DCN neurons

By use of specific blockers our data complement and extend the earlier observations that suggest that SK channels underlie the AHP in DCN neurons (Shakkottai *et al.* 2004). We show that in DCN neurons SK channels are primarily activated by N-type, but not L-, P/Q-, R- or T-type calcium channels.

Interestingly, the neurons of the medial vestibular nucleus, which, like DCN neurons, also receive inputs from the cerebellar cortex, are also selectively sensitive to blockade of K_{Ca} and N-type calcium channels. In these cells, blockade of either channel type reduces the AHP and increases the number of evoked action potentials (Smith *et al.* 2002). Moreover, in neurons of another component of the motor system, the subthalamic nucleus of the basal ganglia, N-type calcium channels significantly contribute to the activation of SK channels (Pineda *et al.* 1998).

Selective coupling of SK channels with specific VGCCs is not uncommon. It has been shown that K_{Ca} channels are activated by calcium influx via closely located calcium channels, probably organized in membrane microdomains (Marrion & Tavalin, 1998; Bloodgood & Sabatini, 2007). In neurons of the suprachiasmatic nucleus, L- and R-type calcium channels are predominantly involved in the AHP generation (Cloues & Sather, 2003), whereas in the dopaminergic neurons of the midbrain, SK channels are selectively activated via T-type calcium channels (Wolfart & Roeper, 2002). Within the cerebellar cortex, Purkinje cell SK channels are exclusively activated by calcium entering through P/Q-type calcium channels (Womack *et al.* 2004).

In this context, the finding that P/Q-type calcium channels do not contribute to intrinsic pacemaking of DCN neurons is informative because episodic ataxia type 2 (EA2) and spinocerebellar ataxia type 6 (SCA6) are caused by mutations that affect the function of these channels (Jodice *et al.* 1997; Zhuchenko *et al.* 1997; Spacey *et al.* 2004). Our data thus support the notion that cerebellar ataxia in EA2 and SCA6 may be primarily the consequence of dysfunction of Purkinje cells (Walter *et al.* 2006). This supposition is further supported by our findings that much higher concentrations of the SK channel activator EBIO are needed to alter the FR of DCN neurons than that used to regulate pacemaking in Purkinje cells. Thus, the efficacy of EBIO in reducing ataxia and episodes of dyskinesia in P/Q-type calcium channel mutant mice is likely to be because of its actions on Purkinje cells.

Presence of other types of cadmium-sensitive calcium-permeable channels

We found a significant difference between the effects of selective block of N-type calcium channels on the firing rate of DCN neurons and that produced by application of cadmium. Moreover, in every cell examined, the application of cadmium or apamin after blockade of N-type calcium channels further increased the firing rate. It is conceivable, but given the very high concentrations of the blockers used perhaps unlikely, that the combination of toxins used did not completely block all the intended calcium channels. However, it is also possible that in addition to N-type calcium channels another cadmium-sensitive calcium entry pathway exists which is coupled to the activation of SK channels. Cellular studies have shown the expression of several calcium channel α subunits in DCN neurons, but there are no published data on characterization of the different calcium currents (aside from a first-pass classification as low- and high-threshold calcium currents; Jahnsen, 1986; Gauck

et al. 2001). Thus, the nature of this additional calcium current remains elusive at present. In addition to the possibility of VGCCs resistant to the toxins and blockers used in this study, the calcium source could also be a member of the transient receptor potential (TRP) channel family. These channels are sensitive to cadmium blockade and are calcium permeable (Inoue *et al.* 2001; Inoue *et al.* 2003), and their expression in the cerebellum includes the cerebellar nuclei (Philipp *et al.* 1998).

DCN neurons and cerebellar function

With the exception of a small portion of the cerebellum, DCN neurons form the output of the cerebellum. Thus, the signals required for motor coordination are encoded in the firing rate of DCN neurons. Here we find that in addition to the channels required for generation of an action potential, two other channels are essential for pacemaking in the majority of DCN neurons examined: a voltage-gated calcium channel which is coupled to a calcium-activated potassium channel. The involvement of these two conductances in regulating pacemaking in DCN neurons is similar to that seen in the principal neurons of the cerebellar cortex, the Purkinje cells. However, although both neurons use SK channels to regulate their interspike interval and thus the regularity of their pacemaking, the high threshold voltage-gated calcium channels that feed the SK channels are N-type in the case of DCN neurons and P/Q-type in case of Purkinje cells.

References

Aizenman CD & Linden DJ (1999). Regulation of the rebound depolarization and spontaneous firing patterns of deep nuclear neurons in slices of rat cerebellum. *J Neurophysiol* **82**, 1697–1709.

Blatz AL & Magleby KL (1986). Single apamin-blocked Ca-activated K^+ channels of small conductance in cultured rat skeletal muscle. *Nature* **323**, 718–720.

Bloodgood BL & Sabatini BL (2007). Nonlinear regulation of unitary synaptic signals by $CaV_{2.3}$ voltage-sensitive calcium channels located in dendritic spines. *Neuron* **53**, 249–260.

Boland LM, Morrill JA & Bean BP (1994). omega-Conotoxin block of N-type calcium channels in frog and rat sympathetic neurons. *J Neurosci* **14**, 5011–5027.

Bond CT, Sprengel R, Bissonnette JM, Kaufmann WA, Pribnow D, Neelands T *et al.* (2000). Respiration and parturition affected by conditional overexpression of the Ca^{2+}-activated K^+ channel subunit, SK3. *Science* **289**, 1942–1946.

Chang CP, Dworetzky SI, Wang J & Goldstein ME (1997). Differential expression of the alpha and beta subunits of the large- conductance calcium-activated potassium channel: implication for channel diversity. *Brain Res Mol Brain Res* **45**, 33–40.

Chung YH, Shin C, Park KH & Cha CI (2000). Immunohistochemical study on the distribution of neuronal voltage-gated calcium channels in the rat cerebellum. *Brain Res* **865**, 278–282.

Cloues RK & Sather WA (2003). Afterhyperpolarization regulates firing rate in neurons of the suprachiasmatic nucleus. *J Neurosci* **23**, 1593–1604.

Czubayko U, Sultan F, Thier P & Schwarz C (2001). Two types of neurons in the rat cerebellar nuclei as distinguished by membrane potentials and intracellular fillings. *J Neurophysiol* **85**, 2017–2029.

Fanelli RJ, McCarthy RT & Chisholm J (1994). Neuropharmacology of nimodipine: from single channels to behavior. *Ann N Y Acad Sci* **747**, 336–350.

Galvez A, Gimenez-Gallego G, Reuben JP, Roy-Contancin L, Feigenbaum P, Kaczorowski GJ & Garcia ML (1990). Purification and characterization of a unique, potent, peptidyl probe for the high conductance calcium-activated potassium channel from venom of the scorpion Buthus tamulus. *J Biol Chem* **265**, 11083–11090.

Gauck V, Thomann M, Jaeger D & Borst A (2001). Spatial distribution of low- and high-voltage-activated calcium currents in neurons of the deep cerebellar nuclei. *J Neurosci* **21**, RC158.

Inoue R, Hanano T, Shi J, Mori Y & Ito Y (2003). Transient receptor potential protein as a novel non-voltage-gated Ca^{2+} entry channel involved in diverse pathophysiological functions. *J Pharmacol Sci* **91**, 271–276.

Inoue R, Okada T, Onoue H, Hara Y, Shimizu S, Naitoh S *et al.* (2001). The transient receptor potential protein homologue TRP6 is the essential component of vascular α_1-adrenoceptor-activated Ca^{2+}-permeable cation channel. *Circ Res* **88**, 325–332.

Ito M (1984). *The Cerebellum and Neural Control*. Raven Press, New York.

Jahnsen H (1986). Electrophysiological characteristics of neurones in the guinea-pig deep cerebellar nuclei *in vitro*. *J Physiol* **372**, 129–147.

Jodice C, Mantuano E, Veneziano L, Trettel F, Sabbadini G, Calandriello L *et al.* (1997). Episodic ataxia type 2 (EA2) and spinocerebellar ataxia type 6 (SCA6) due to CAG repeat expansion in the CACNA1A gene on chromosome 19p. *Hum Mol Genet* **6**, 1973–1978.

McCleskey EW, Fox AP, Feldman DH, Cruz LJ, Olivera BM, Tsien RW & Yoshikami D (1987). Omega-conotoxin: direct and persistent blockade of specific types of calcium channels in neurons but not muscle. *Proc Natl Acad Sci U S A* **84**, 4327–4331.

McDonough SI & Bean BP (1998). Mibefradil inhibition of T-type calcium channels in cerebellar purkinje neurons. *Mol Pharmacol* **54**, 1080–1087.

Marrion NV & Tavalin SJ (1998). Selective activation of Ca^{2+}-activated K^+ channels by co-localized Ca^{2+} channels in hippocampal neurons. *Nature* **395**, 900–905.

Martin RL, Lee JH, Cribbs LL, Perez-Reyes E & Hanck DA (2000). Mibefradil block of cloned T-type calcium channels. *J Pharmacol Exp Ther* **295**, 302–308.

Mintz IM, Venema VJ, Swiderek KM, Lee TD, Bean BP & Adams ME (1992). P-type calcium channels blocked by the spider toxin omega-Aga-IVA. *Nature* **355**, 827–829.

Molineux ML, McRory JE, McKay BE, Hamid J, Mehaffey WH, Rehak R *et al.* (2006). Specific T-type calcium channel isoforms are associated with distinct burst phenotypes in deep cerebellar nuclear neurons. *Proc Natl Acad Sci U S A* **103**, 5555–5560.

Newcomb R, Szoke B, Palma A, Wang G, Chen X, Hopkins W *et al.* (1998). Selective peptide antagonist of the class E calcium channel from the venom of the tarantula *Hysterocrates gigas*. *Biochemistry* **37**, 15353–15362.

Pedarzani P, Mosbacher J, Rivard A, Cingolani LA, Oliver D, Stocker M *et al.* (2001). Control of electrical activity in central neurons by modulating the gating of small conductance Ca^{2+}-activated K^+ channels. *J Biol Chem* **276**, 9762–9769.

Philipp S, Hambrecht J, Braslavski L, Schroth G, Freichel M, Murakami M *et al.* (1998). A novel capacitative calcium entry channel expressed in excitable cells. *EMBO J* **17**, 4274–4282.

Pineda JC, Waters RS & Foehring RC (1998). Specificity in the interaction of HVA Ca^{2+} channel types with Ca^{2+}-dependent AHPs and firing behavior in neocortical pyramidal neurons. *J Neurophysiol* **79**, 2522–2534.

Puopolo M, Bean BP & Raviola E (2005). Spontaneous activity of isolated dopaminergic periglomerular cells of the main olfactory bulb. *J Neurophysiol* **94**, 3618–3627.

Puopolo M, Raviola E & Bean BP (2007). Roles of subthreshold calcium current and sodium current in spontaneous firing of mouse midbrain dopamine neurons. *J Neurosci* **27**, 645–656.

Raman IM, Gustafson AE & Padgett D (2000). Ionic currents and spontaneous firing in neurons isolated from the cerebellar nuclei. *J Neurosci* **20**, 9004–9016.

Reynolds IJ, Wagner JA, Snyder SH, Thayer SA, Olivera BM & Miller RJ (1986). Brain voltage-sensitive calcium channel subtypes differentiated by omega-conotoxin fraction GVIA. *Proc Natl Acad Sci U S A* **83**, 8804–8807.

Sailer CA, Kaufmann WA, Marksteiner J & Knaus HG (2004). Comparative immunohistochemical distribution of three small-conductance Ca^{2+}-activated potassium channel subunits, SK1, SK2, and SK3 in mouse brain. *Mol Cell Neurosci* **26**, 458–469.

Sausbier M, Hu H, Arntz C, Feil S, Kamm S, Adelsberger H *et al.* (2004). Cerebellar ataxia and Purkinje cell dysfunction caused by Ca^{2+}-activated K^+ channel deficiency. *Proc Natl Acad Sci U S A* **101**, 9474–9478.

Shakkottai VG, Chou CH, Oddo S, Sailer CA, Knaus HG, Gutman GA *et al.* (2004). Enhanced neuronal excitability in the absence of neurodegeneration induces cerebellar ataxia. *J Clin Invest* **113**, 582–590.

Smith MR, Nelson AB & Du LS (2002). Regulation of firing response gain by calcium-dependent mechanisms in vestibular nucleus neurons. *J Neurophysiol* **87**, 2031–2042

Spacey SD, Hildebrand ME, Materek LA, Bird TD & Snutch TP (2004). Functional implications of a novel EA2 mutation in the P/Q-type calcium channel. *Ann Neurol* **56**, 213–220.

Stocker JW, Nadasdi L, Aldrich RW & Tsien RW (1997). Preferential interaction of omega-conotoxins with inactivated N-type Ca^{2+} channels. *J Neurosci* **17**, 3002–3013.

Stone TW (1993). Neuropharmacology of quinolinic and kynurenic acids. *Pharmacol Rev* **45**, 309–379.

Tanaka O, Sakagami H & Kondo H (1995). Localization of mRNAs of voltage-dependent Ca^{2+}-channels: four subtypes of a1- and b-subunits in developing and mature rat brain. *Brain Res Mol Brain Res* **30**, 1–16.

Tottene A, Volsen S & Pietrobon D (2000). α_{1E} Subunits form the pore of three cerebellar R-type calcium channels with different pharmacological and permeation properties. *J Neurosci* **20**, 171–178.

Uusisaari M, Obata K & Knopfel T (2007). Morphological and electrophysiological properties of GABAergic and non-GABAergic cells in the deep cerebellar nuclei. *J Neurophysiol* **97**, 901–911.

Volsen SG, Day NC, McCormack AL, Smith W, Craig PJ, Beattie R *et al.* (1995). The expression of neuronal voltage-dependent calcium channels in human cerebellum. *Brain Res Mol Brain Res* **34**, 271–282.

Walter JT, Alviña K, Womack MD, Chevez C & Khodakhah K (2006). Decreases in the precision of Purkinje cell pacemaking cause cerebellar dysfunction and ataxia. *Nat Neurosci* **9**, 389–397.

Wolfart J & Roeper J (2002). Selective coupling of T-type calcium channels to SK potassium channels prevents intrinsic bursting in dopaminergic midbrain neurons. *J Neurosci* **22**, 3404–3413.

Womack MD, Chevez C & Khodakhah K (2004). Calcium-activated potassium channels are selectively coupled to P/Q-type calcium channels in cerebellar Purkinje neurons. *J Neurosci* **24**, 8818–8822.

Womack M & Khodakhah K (2002). Active contribution of dendrites to the tonic and trimodal patterns of activity in cerebellar purkinje neurons. *J Neurosci* **22**, 10603–10612.

Womack MD & Khodakhah K (2003). Somatic and dendritic small-conductance calcium-activated potassium channels regulate the output of cerebellar purkinje neurons. *J Neurosci* **23**, 2600–2607.

Yoon KW, Covey DF & Rothman SM (1993). Multiple mechanisms of picrotoxin block of GABA-induced currents in rat hippocampal neurons. *J Physiol* **464**, 423–439.

Zhuchenko O, Bailey J, Bonnen P, Ashizawa T, Stockton DW, Amos C *et al.* (1997). Autosomal dominant cerebellar ataxia (SCA6) associated with small polyglutamine expansions in the a1A-voltage-dependent calcium channel. *Nat Genet* **15**, 62–69.

Supplemental material

Online supplemental material for this paper can be accessed at:
http://jp.physoc.org/cgi/content/full/jphysiol.2007.148197/DC1
and
http://www.blackwell-synergy.com/doi/suppl/10.1113/jphysiol.2007.148197